

## Efficient synthesis of the Cu-SSZ-39 catalyst for DeNO<sub>x</sub> applications

Nuria Martín, Manuel Moliner,\* Avelino Corma\*

Instituto de Tecnología Química (UPV-CSIC), Universidad Politécnica de Valencia,  
Consejo Superior de Investigaciones Científicas, Valencia, 46022, Spain

\*Corresponding authors: E-mail addresses: [acorma@itq.upv.es](mailto:acorma@itq.upv.es); [mmoliner@itq.upv.es](mailto:mmoliner@itq.upv.es)

The use of small pore zeolites with large cavities has been reported for relevant applications in catalysis or gas separation.<sup>[1]</sup> One of the most important applications of these materials as catalysts is the selective catalytic reduction (SCR) of nitrogen oxides (NO<sub>x</sub>), where copper-containing zeolites with small pore sizes show excellent activities to remove these hazardous compounds produced during combustion in diesel engines.<sup>[1,2]</sup> Interestingly, these small-pore zeolites show higher hydrothermal stability compared to other zeolitic materials presenting larger pore sizes, such as Cu-ZSM-5 or Cu-Beta.<sup>[3]</sup> The particular stabilization of the Cu<sup>2+</sup> cations within the double 6-rings (D6Rs) present in some structures of these small pore zeolites, i.e. chabazite (CHA structure), has been claimed as a plausible reason for their higher hydrothermal stability.<sup>[4]</sup>

Another zeolite with related structural properties to chabazite is SSZ-39 (AEI structure), which is an aluminosilicate with large cages connected by a three-directional small 8-ring (8-R) pore system, and also with D6R as secondary building units in its structure.<sup>[5]</sup> Recently, we have reported that Cu-exchanged SSZ-39 zeolite is an active and hydrothermally stable catalyst for the SCR of NO<sub>x</sub> with ammonia, showing even better catalytic performance than Cu-exchanged CHA.<sup>[6]</sup>

The preferred synthesis procedure of SSZ-39 requires the use of simple alkyl-substituted cyclic quaternary ammonium cations as organic structure directing agents (OSDAs) in alkaline conditions.<sup>[7]</sup> These organic cations could be easily prepared from commercially-available pyridine precursors,<sup>[8]</sup> making attractive the use of these OSDAs for the synthesis of the SSZ-39 from an economic point of view. Unfortunately, this methodology can afford the preparation of the SSZ-39 in low solid yields (lower than 50%), since the final crystalline solids show much lower Si/Al ratios than the Si/Al ratios initially introduced in the synthesis gels,<sup>[6,7,8]</sup> indicating that most of the Si species remain in solution after the crystallization procedure. This fact limits the potential use of SSZ-39 in commercial applications.

Recently, the synthesis of the high silica AEI zeolite with high solid yields (above 80%) has been reported using USY zeolite as silicon source and tetraethylphosphonium (TEP) cations as OSDA.<sup>[9]</sup> Although this achievement is highly relevant in terms of the optimization of the SSZ-39 synthesis, the use of P-based OSDAs still presents some

important drawbacks. On one hand, phosphine-derived organic molecules show important environmental and health hazards, and, on the other hand, the complete removal of the phosphorous-species entrapped within the zeolitic cavities is very difficult, especially within small pore zeolites, and their calcination process requires high temperatures and hydrogen atmospheres for the complete decomposition/elimination of these compounds.<sup>[9]</sup>

It is worth mentioning that in the last years the use of pre-formed crystalline zeolitic precursors to synthesize different zeolites through *zeolite to zeolite* transformations has attracted much attention.<sup>[10]</sup> The reason for that is because these crystalline sources can intensely change the nucleation/crystallization driving forces compared to other amorphous silicoaluminate precursors.<sup>[11]</sup> Indeed, these crystalline precursors will show lower dissolution rates towards monomeric or low polymeric species in the synthesis gels, favoring the presence of very small crystalline species that will act as catalysts for increasing the nucleation/crystallization rates or directing the crystallization of a different zeolite.<sup>[10,11]</sup>

If this is so, it could also be expected that the lower dissolution rates observed for crystalline molecular sieves acting as Si and Al sources, could preclude the excessive dissolution towards monomeric silicate species that would remain in solution, favoring the efficient synthesis of SSZ-39 with high solid yields when combined with simple alkyl-substituted cyclic quaternary ammonium cations acting as OSDAs, such as N,N-dimethyl-3,5-dimethylpiperidinium.

Herein, we propose a synthesis method to achieve the SSZ-39 with high solid yields based on *zeolite to zeolite* transformation using high-silica USY zeolite (FAU) as a silicon and aluminum source that avoids the use of phosphine-derived cations. We have found that through this system method it is possible to prepare highly active and hydrothermally stable catalysts for the SCR of NO<sub>x</sub>, introducing copper ions into the zeolite SSZ-39 by either a post-synthetic ion exchange or by “one-pot” method based on the cooperative effect of the N,N-dimethyl-3,5-dimethylpiperidinium and the Cu-tetraethylenepentamine (Cu-TEPA) complex as OSDAs.

SSZ-39 has been synthesized by hydrothermal conversion of commercial FAU (CBV-720 with SiO<sub>2</sub>/Al<sub>2</sub>O<sub>3</sub> ratio of 21) in the presence of N,N-dimethyl-3,5-dimethylpiperidinium as OSDA and sodium hydroxide. The synthesis gel shows the following chemical composition: SiO<sub>2</sub>/0.047Al<sub>2</sub>O<sub>3</sub>/0.2NaOH/0.2OSDA/15H<sub>2</sub>O, and the crystallization takes place at 135°C for 7 days. The powder X-Ray diffraction pattern (PXRD) of the final solids indicates the crystallization of the SSZ-39 material as pure phase (see N-SSZ-39 in Figure 1) and, remarkably, the final solid yield achieved is above 80% (without taking into account the organic moieties).

The textural properties of the calcined N-SSZ-39 sample have been studied by N<sub>2</sub> adsorption. The N<sub>2</sub> adsorption isotherm at 77 K shown in Figure XXX reveals the high microporous nature of this material. The calculated BET (Brunauer-Emmett-Teller) surface area and the micropore area for this calcined material are XXXX and XXXX m<sup>2</sup>/g, respectively, while the micropore volume is XXX cm<sup>3</sup>/g. On the other hand, scanning electron microscopy (SEM) images indicates the formation of small cubic crystallites in N-SSZ-39 sample (0.3-0.4 μm, see Figure 2a), and chemical analysis of the N-SSZ-39 zeolite shows a Si/Al ratio of 8.2 (see Table 1). Characterization of the as-prepared and calcined N-SSZ-39 samples by <sup>27</sup>Al MAS NMR spectroscopy (see Figure 3), shows a single peak centered at ~ 55 ppm in both N-SSZ-39 samples, indicating that aluminum species are placed in tetrahedral coordination in the AEI framework, even after being calcined in air at 580°C.

For comparison purposes, we have also prepared a high-silica SSZ-39 zeolite using tetraethylphosphonium cations as OSDA, following the procedure described by Maruo et al.<sup>[9]</sup> The chemical molar ratios of the synthesis gel were SiO<sub>2</sub>/0.045Al<sub>2</sub>O<sub>3</sub>/0.1NaOH/0.2OSDA/5H<sub>2</sub>O, and the crystallization was conducted at 150°C for 9 days. The PXRD pattern shows the formation of the SSZ-39 material as a pure phase (see P-SSZ-39 in Figure 1). Chemical analysis of this sample reveals a Si/Al ratio of 8.4 (see Table 1), which is very similar to the Si/Al ratio obtained for our N-SSZ-39 material (8.0, see Table 1). Scanning electron microscopy (SEM) images of P-SSZ-39 show the presence of small crystals of ~ 0.1 μm with a cubic morphology (see Figure 2b).

To properly remove the phosphorous-containing OSDAs entrapped within the pores of the as-prepared P-SSZ-39 material, the sample has to be calcined under a hydrogen atmosphere at 800°C for 4h.<sup>[9]</sup> The <sup>27</sup>Al MAS NMR spectrum of the calcined P-SSZ-39 material shows in addition to the band centered at 55 ppm, which has been assigned to tetrahedrally coordinated Al species, the presence of other bands centered at 45 and 0 ppm, which have been assigned to pentacoordinated and octahedrally coordinated extra-framework Al, respectively (see P-SSZ-39\_Calc in Figure 3). Thus, it seems that the severe calcination treatment required to remove the P species entrapped within the AEI cavities, results in the extraction from framework positions of part of the Al species.

As it has been mentioned above, Cu containing zeolites with small pore size, such as the case of the SSZ-39 (AEI) zeolite, are very active for the SCR of NO<sub>x</sub>.<sup>[1]</sup> Thus, in order to evaluate and compare the catalytic activity of N-SSZ-39 and P-SSZ-39 samples, Cu<sup>2+</sup> species must be introduced in these calcined samples. The Al species that remain in tetrahedral coordination after the calcination procedures generate negative charges in the zeolitic framework that would allow the introduction and stabilization of extra-framework cations, such as Cu<sup>2+</sup>. In this case, the Cu<sup>2+</sup> species have been introduced by a post-synthetic cation-exchange procedure within both calcined SSZ-39 materials, using an aqueous solution of Cu(CH<sub>3</sub>COO)<sub>2</sub> (see experimental section). Chemical analyses indicate that the metal content introduced within both catalysts is very similar (4.7 and 4.6%wt for Cu-N-SSZ-39 and Cu-P-SSZ-39, respectively, see Table 1).

These Cu-exchanged SSZ-39 catalysts have been tested for the SCR of NO<sub>x</sub> catalytic reaction using NH<sub>3</sub> as reductor. The conditions for the catalytic test include a reaction feed composed by 500 ppm of NO, 500 ppm of NH<sub>3</sub>, 5% of water and 7% of O<sub>2</sub>, a wide range of reaction temperatures (170-550°C), and a very high gas hourly space velocity of 450,000 ml/h.g<sub>cat</sub>. As it can be seen in Figure 4, Cu-N-SSZ-39 catalyst shows a significant higher catalytic activity compared to Cu-P-SSZ-39 under most of the tested reaction temperatures. Indeed, Cu-N-SSZ-39 catalyst achieves NO conversion values above 90% in a very broad range of temperatures (250-500°C), while Cu-P-SSZ-39 only reaches NO conversion values close to 90% under temperatures comprised between 350 and 400°C.

These Cu-containing SSZ-39 catalysts have been characterized by temperature-programmed reduction (TPR) using hydrogen in order to perform a preliminary study of the possible Cu species present in the catalysts. According to the literature, the signals observed for the H<sub>2</sub> consumption peaks at temperatures from 200 to 500°C in related Cu-containing zeolites are associated to different species of copper in the catalysts.<sup>[12]</sup> Indeed, the signals associated to the reduction of Cu<sup>2+</sup>, bulk CuO and Cu<sup>+</sup> species have been reported for 250-270°C, 350-370°C, and 400-450°C, respectively.<sup>[12]</sup> As it can be seen in Figure 5, Cu-N-SSZ-39 catalyst shows the main presence of two bands below 300°C, which could be assigned to the preferential presence of Cu<sup>2+</sup> species, probably under two different crystallographic environments within the AEI cavities. On the other hand, Cu-P-SSZ-39 also presents these two bands below 300°C corresponding to Cu<sup>2+</sup> species, but in addition, a broad band between 300 and 500°C reveals the presence of other Cu species, probably a combination of bulk CuO and Cu<sup>+</sup> species (see Figure 5). This different distribution of Cu species in both catalysts could be explained by the different Al coordination found by <sup>27</sup>Al MAS NMR spectroscopy (see Figure 3), indicating a significant lower stabilization of the extra-framework Cu<sup>2+</sup> species within Cu-P-SSZ-39 catalyst due to the lower presence of tetrahedrally coordinated Al species. This heterogeneous metal distribution through the Cu-P-SSZ-39 catalyst also explains its lower catalytic behavior for SCR of NO<sub>x</sub> compared to Cu-N-SSZ-39 (see Figure 4).

Both catalysts have been treated in the presence of steam at 750°C for 13h in order to study their hydrothermal stability under severe conditions. As seen in Figure 1, the Cu-N-SSZ-39 catalyst preserves its crystalline structure, while the structure of Cu-P-SSZ-39 catalyst collapses after the harsh ageing steaming (see PXRD patterns of Cu-N-SSZ-39-HT and Cu-P-SSZ-39-HT, respectively). This result confirms the remarkably higher hydrothermal stability of the Cu-containing SSZ-39 catalyst synthesized using the simple cyclic ammonium cation compared to the phosphonium cation as OSDAs. Interestingly, the aged Cu-N-SSZ-39-HT catalyst performs very well for SRC of NO<sub>x</sub>, achieving NO conversion values above 90% at reaction temperatures between 250 and 450°C (see Figure 4).

Recently, it has been described the direct synthesis of Cu-SSZ-13<sup>[13]</sup> and other related Cu-containing silicoaluminophosphate materials, such as Cu-SAPO-34<sup>[12d],[14]</sup> and Cu-

SAPO-18,<sup>[15]</sup> using the combination of an organometallic Cu-complex (Cu-TEPA) and a cooperative organic molecule as OSDA. Following a similar “one-pot” synthesis procedure combining Cu-TEPA and N,N-dimethyl-3,5-dimethylpiperidinium as cooperative OSDAs, a crystalline Cu-containing SSZ-39 material has been achieved (see supporting information for experimental details and the PXRD pattern of Cu-SSZ-39 in Figure 1). The yield of the synthesis is very high (above 90%), and the chemical analysis reveals a Si/Al ratio of almost 10 and a Cu content of 3.3wt%. Interestingly, the Cu-TEPA complex remains intact during the zeolite crystallization, as revealed by the single band centered at 260 nm present in the UV-Vis spectrum of the as-prepared Cu-SSZ-39 material (see Figure 6). The sample has been calcined in air at 550°C for four hours to remove the organic moieties precluded within the AEI structure, and the catalytic activity of this Cu-SSZ-39 was evaluated for SCR of NO<sub>x</sub>. As seen in Figure 4, the Cu-SSZ-39 sample synthesized by the “one-pot” methodology shows NO conversion values above 90% for reaction temperatures comprised between 250 and 450°C, as the optimum Cu-exchanged SSZ-39 catalyst described above. The one-pot Cu-SSZ-39 catalyst has also been characterized by H<sub>2</sub>-TPR, observing that the H<sub>2</sub> consumption occurs preferentially below 300°C, which can be assigned to the main presence of Cu<sup>2+</sup> species within the catalyst (see Cu-SSZ-39 in Figure 5).

In summary, the synthesis of the high-silica SSZ-39 zeolite with high-solid yields has been accomplished by combining the use of USY as crystalline Si and Al source and N,N-dimethyl-3,5-dimethylpiperidinium as simple OSDA, avoiding the use of P-derived templates. A “one-pot” synthesis using Cu-TEPA and N,N-dimethyl-3,5-dimethylpiperidinium as OSDAs can yield Cu-SSZ-39 with solid yields above 90%. Both Cu-SSZ-39 materials, prepared by one-pot or Cu ion-exchange methods, are excellent catalysts for the SCR of NO<sub>x</sub>.

### **Acknowledgments**

Financial support by the Spanish Government-MINECO through “Severo Ochoa” (SEV 2012-0267), Consolider Ingenio 2010-Multicat, MAT2012-37160 and, Intramural-201480I015 is acknowledged. The authors thank Isabel Millet for technical support.

**Figure 1: PXRD patterns of N-SSZ-39 and P-SSZ-39 materials**

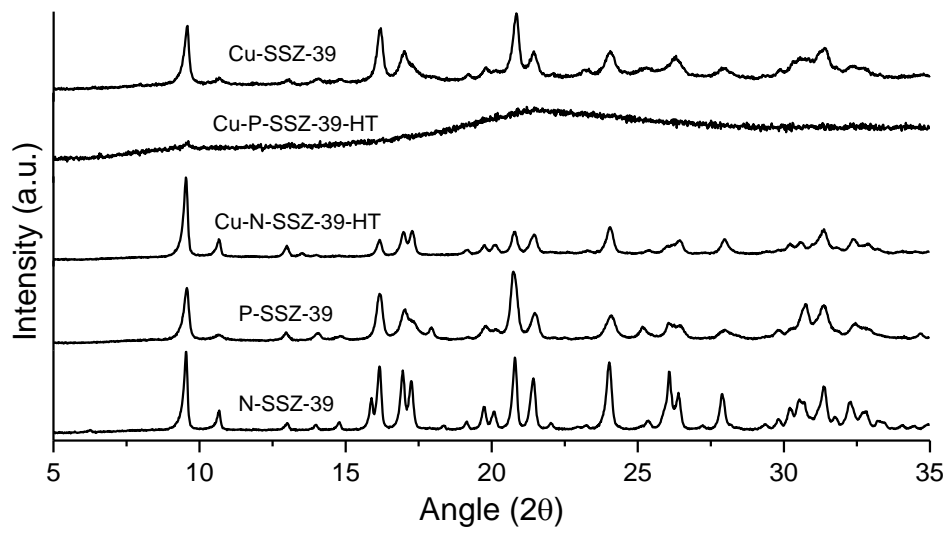




Figure 2: SEM images of a) N-SSZ-39 y b) P-SSZ-39

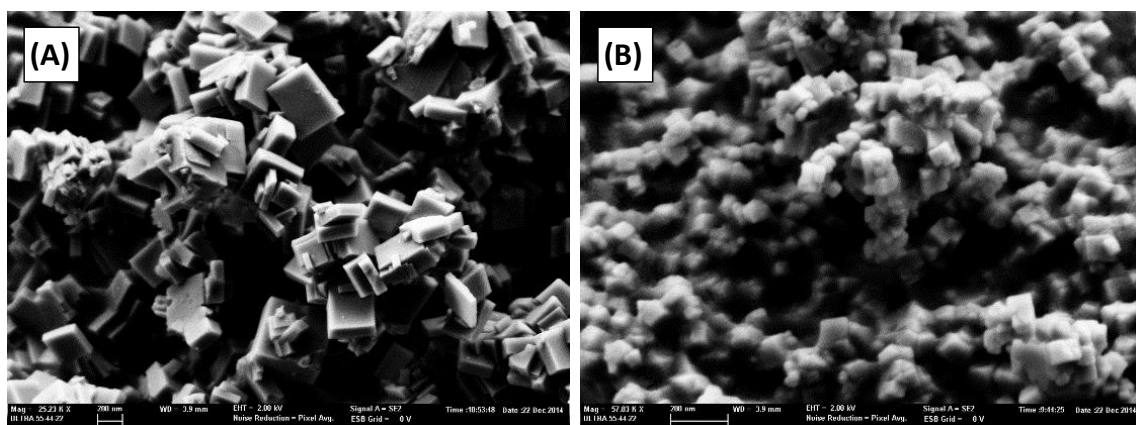
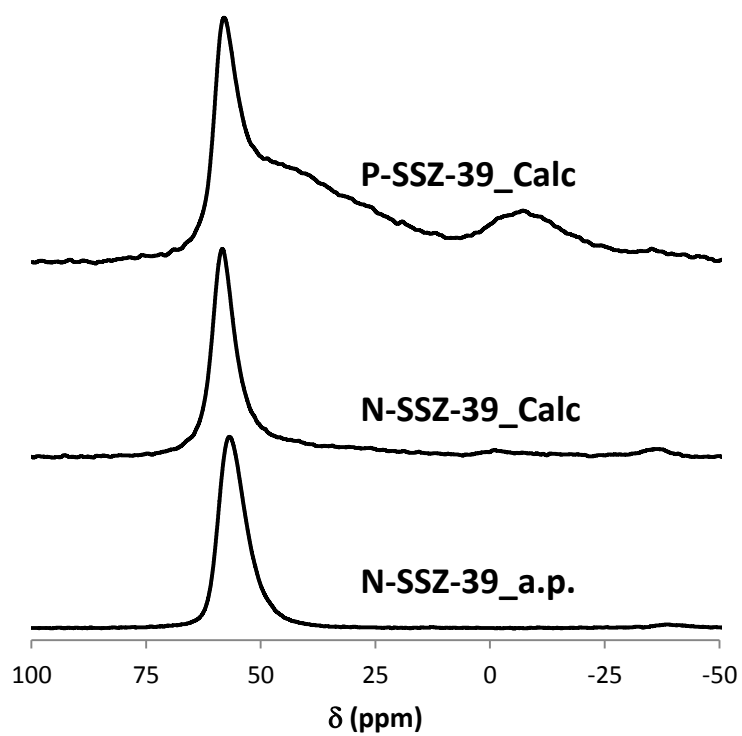


Figure 3:  $^{27}\text{Al}$  MAS NMR spectra of SSZ-39 materials



**Figure 4: Catalytic activity for the NH<sub>3</sub>-SCR of NO<sub>x</sub> reaction of the different Cu-SSZ-39 materials under severe reaction conditions in the presence of water and very high space velocity (450,000 ml/h.gcat)**

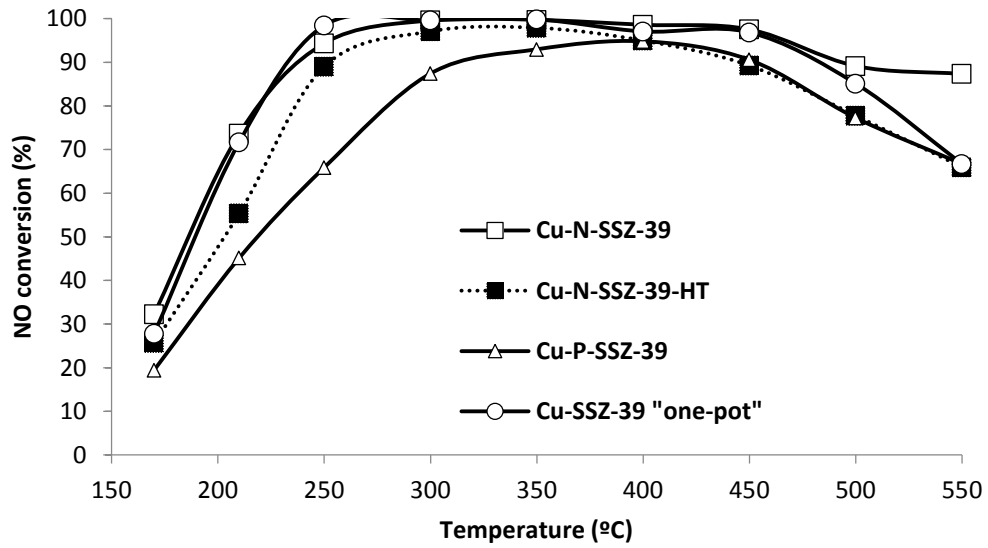
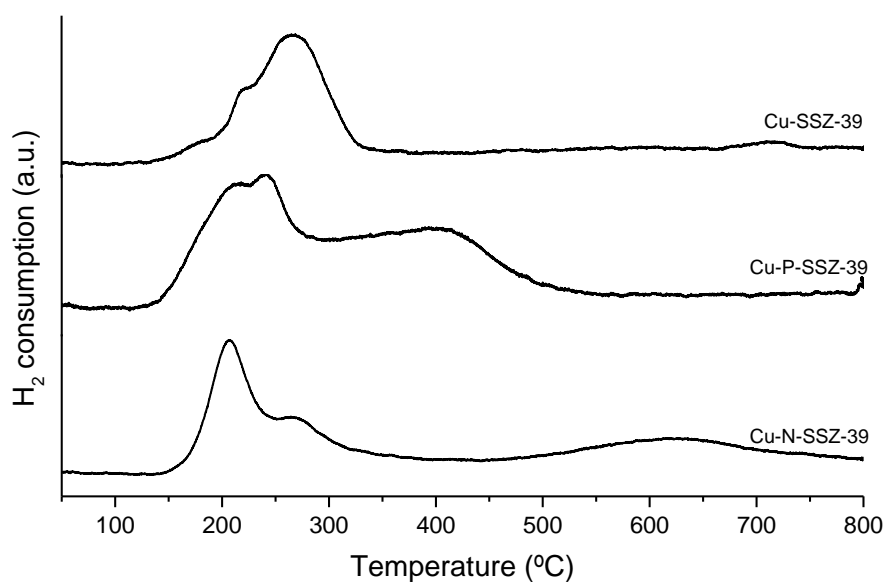
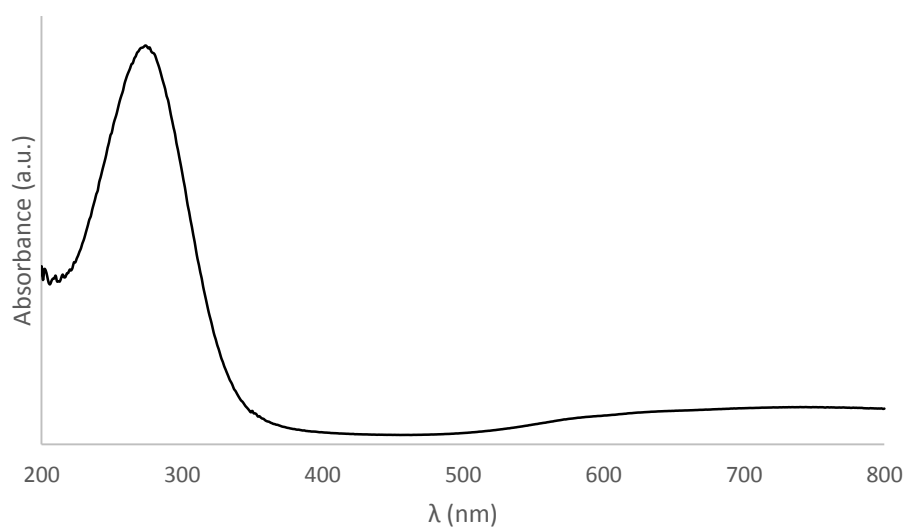


Figure 5: H<sub>2</sub>-TPR profile of calcined Cu-containing SSZ-39 samples



**Figure 6: UV-Vis spectrum of the as-prepared Cu-SSZ-39 material**



**Table 1: ICP analyses of the zeolitic samples**

<i>Sample</i>	<i>Si/Al</i>	<i>%wt Cu</i>
<i>N-SSZ-39</i>	8.2	---
<i>P-SSZ-39</i>	8.4	---
<i>Cu-N-SSZ-39</i>	8.1	4.7
<i>Cu-P-SSZ-39</i>	8.5	4.6
<i>Cu-SSZ-39</i>	9.9	3.3

## SUPPLEMENTARY MATERIAL

### 1.- OSDA and zeolite syntheses

#### Synthesis of OSDA N, N-dimethyl-3, 5-dimethylpiperidinium

10 g of 3,5-dimethylpiperidine ( $C_7H_{15}$ , Acros Organics, 96%, cis-trans mixture) was mixed with 140 mL of methanol ( $CH_3OH$ , Scharlab, 99.9%) and 19.51 g of potassium carbonate ( $KHCO_3$ , Sigma Aldrich, 99.7%). While this mixture was stirred, 54 g of methyl iodide ( $CH_3I$ , Sigma Aldrich, 99.9%) was added dropwise. The reaction was stirred for 7 days. After this time, MeOH was partially removed under vacuum, and the iodide salt was precipitated by addition of diethyl ether. For its use in the synthesis of zeolites, the final product was ion exchanged to the hydroxide form using a commercially available hydroxide ion exchange resin (Dowex SBR).

#### Synthesis of SSZ-39 zeolite using FAU zeolite as silicon and aluminum source and N, N-dimethyl-3,5-dimethylpiperidinium hydroxide as OSDA

The hydrothermal synthesis of AEI zeolite was carried out as follows. First the OSDA N,N-dimethyl-3,5-dimethylpiperidinium hydroxide was mixed with a 20%wt aqueous solution of sodium hydroxide (NaOH granulated, Scharlab). Then, the crystals of USY zeolite (CBV-720 with  $SiO_2/Al_2O_3=21$ ) were introduced in this solution. The mixture was stirred until complete homogenization of the gel. The chemical composition of the synthesis gel was  $SiO_2/0.045Al_2O_3/0.2NaOH/0.2OSDA/15H_2O$ . The resultant gel was transferred into a stainless steel autoclave with a Teflon liner. The crystallization was then conducted at 135°C for 7 days under static conditions. The solid product was filtered, washed with water and dried at 100°C. Finally, the sample was calcined in air at 550°C for 4h.

#### Synthesis of SSZ-39 zeolite using FAU zeolite as silicon and aluminum source and tetraethyl phosphonium hydroxide as OSDA

Phosphorous-containing SSZ-39 zeolite has been synthesized according to the method reported by Maruo et al.<sup>[9]</sup> The chemical composition of the synthesis gel was  $SiO_2/0.045Al_2O_3/0.1NaOH/0.2OSDA/5H_2O$ , where OSDA corresponds to tetraethyl

phosphonium hydroxide. The crystallization was conducted at 150°C for 9 days under static conditions. The solid product was filtered, washed with water and dried at 100°C. Finally, the sample was calcined under a hydrogen atmosphere at 800°C for 4h to assure the complete decomposition of the phosphorous-containing species.

#### Post-synthetic Cu-exchange procedure on N-SSZ-39 and P-SSZ-39 materials

In order to perform the Cu ion exchange on the calcined SSZ-39 materials, the samples were exchanged with the required amount of a  $\text{Cu}(\text{CH}_3\text{CO}_2)_2$  solution (solid/liquid ratio of 10g/L) at room temperature for 10 hours. Finally, the samples were filtered and washed with distilled water, and calcined in air at 550°C for 4 h.

#### “One-pot” synthesis procedure of Cu-SSZ-39

The one-pot synthesis of Cu-SSZ-39 was prepared using a mixture of Cu-TEPA complex and N,N-dimethyl-3,5-dimethylpiperidinium as cooperative OSDAs. First, the Cu-TEPA complex was in-situ prepared by mixing a 20wt% aqueous solution of copper (II) sulfate ( $\text{CuSO}_4$ , Alfa Aesar, 98%) with the required amount of tetraethylenepentamine (TEPA, 98%, Sigma Aldrich). This mixture was stirred for 2 h. Then, aqueous solutions of the OSDA N-dimethyl-3,5-dimethylpiperidinium hydroxide and sodium hydroxide were added to the above Cu-TEPA solution. Finally, crystals of USY (CBV-720,  $\text{SiO}_2/\text{Al}_2\text{O}_3=21$ ) were introduced as Si and Al sources to the mixture. The final composition of the synthesis gel was the following:  $\text{SiO}_2$  / 0.045  $\text{Al}_2\text{O}_3$  / 0.05 Cu-TEPA / 0.4 OSDA / 0.2 NaOH / 25  $\text{H}_2\text{O}$ . This gel was transferred to an autoclave with a Teflon liner and heated at 135°C under static conditions. The final solids were recovered and washed by filtration. The sample was calcined at 550°C in air for 4 hours to remove the organic species.

## **2.- Characterization**

Powder X-ray diffraction (PXRD) measurements were performed with a multisample Philips X'Pert diffractometer equipped with a graphite monochromator, operating at 45 kV and 40 mA, and using Cu K $\alpha$  radiation ( $\lambda = 0,1542$  nm).

The chemical analyses were carried out in a Varian 715-ES ICP-Optical Emission spectrometer, after solid dissolution in  $\text{HNO}_3/\text{HCl}/\text{HF}$  aqueous solution. The organic



content of the as-made materials was determined by elemental analysis performed with a SCHN FISIONS elemental analyzer.

The morphology of the samples was studied by field emission scanning electron microscopy (FESEM) using a ZEISS Ultra-55 microscope

$^{27}\text{Al}$  MAS NMR spectra were recorded at room temperature with a Bruker AV 400 spectrometer at 104.2 MHz with a spinning rate of 10 kHz and  $9^\circ$  pulse length of 0.5  $\mu\text{s}$  with a 1 s repetition time.  $^{27}\text{Al}$  chemical shift was referred to  $\text{Al}^{3+}(\text{H}_2\text{O})_6$ .

Temperature programmed reduction (TPR) experiments were performed in a Micromeritics Autochem 2910 equipment.

### **3.- Catalytic experiments**

The activity of the samples for the selective catalytic reduction (SCR) of  $\text{NO}_x$  using  $\text{NH}_3$  as reductor was tested in a fixed bed, quartz tubular reactor of 1.2 cm of diameter and 20 cm length. The total gas flow was fixed at 300 ml/min, containing 500 ppm of  $\text{NO}$ , 530 ppm of  $\text{NH}_3$ , 7% of  $\text{O}_2$ , and 5% of  $\text{H}_2\text{O}$ . The catalyst (40 mg) was introduced in the reactor, heated up to 550  $^\circ\text{C}$  and maintained at this temperature for one hour under nitrogen flow. Then, the desired reaction temperature was set (170-550 $^\circ\text{C}$ ) and the reaction feed admitted. The  $\text{NO}_x$  present in the outlet gases from the reactor were analyzed continuously by means of a chemiluminescence detector (Thermo 62C).

## References

---

- [1] Moliner, M.; Martínez, C.; Corma, A. *Chem. Mater.*, **2014**, *26*, 246-258.
- [2] Brandenberger, S.; Kröcher, O.; Tissler, A.; Althoff, R. *Catal. Rev. Sci. Eng.*, **2008**, *50*, 492-531.
- [3] (a) Bull, I.; Boorse, R. S.; Jaglowski, W. M.; Koermer, G. S.; Moini, A.; Patchett, J. A.; Xue, W. M.; Burk, P.; Dettling, J. C.; Caudle, M. T. *U.S. Patent 0226545*, **2008**; (b) Fickel, D. W.; D'Addio, E.; Lauterbach, J. A.; Lobo, R. F. *Appl. Catal. B*, **2011**, *102*, 441-448; (c) Kwak, J. H.; Tonkyn, R. G.; Kim, D. H.; Szanyi, J.; Peden, C. H. F. *J. Catal.*, **2010**, *275*, 187.
- [4] Fickel, D. W.; Lobo, R. F. *J. Phys. Chem. C*, **2010**, *114*, 1633-1640.
- [5] Wagner, P.; Nakagawa, Y.; Lee, G. S.; Davis, M. E.; Elomari, S.; Medrud, R. C.; Zones, S. I. *J. Am. Chem. Soc.*, **2000**, *122*, 263-273.
- [6] Moliner, M.; Franch, C.; Palomares, E.; Grill, M.; Corma, A. *Chem. Commun.* **2012**, *48*, 8264-8266.
- [7] Zones, S. I.; Nakagawa, Y.; Evans, S. T., Lee, G. S. *U.S. Patent 5958370*, **1999**.
- [8] Davis et al. REF SSZ-39.
- [9] (a) Maruo, T.; Yamanaka, N.; Tsunoji, N.; Sadakane, M.; Sano, T. *Chem. Lett.*, **2014**, *43*, 302-304; (b) Sonoda, T.; Maruo, T.; Yamasaki, Y.; Tsunoji, N.; Takamitsu, Y.; Sadakane, M.; Sano, T. *J. Mater. Chem. A*, **2015**, *3*, 857.
- [10] Sano, T.; Itakura, M.; Sadakane, M. *J. Jap. Pet. Inst.*, **2013**, *56*, 183-197.
- [11] (a) Yashiki, A.; Honda, K.; Fujimoto, A.; Shibata, S.; Ide, Y.; Sadakane, M.; Sano, T. *J. Cryst. Growth*, **2011**, *325*, 96-100; (b) Jon, H.; Nakahata, K.; Lu, B.; Oumi, Y., Sano, T. *Micropor. Mesopor. Mater.*, **2006**, *96*, 72-78; (c) Goto, I.; Itakura, M.; Shibata, S.; Honda, K.; Ide, Y.; Sadakane, M., Sano, T. *Micropor. Mesopor. Mater.*, **2012**, *158*, 117-122.
- [12] (a) Wang, J.; Yu, T.; Wang, X.; Qi, G.; Xue, J.; Shen, M.; Li, W. *Appl. Catal. B.*, **2012**, *127*, 137; (b) Wan, Y.; Ma, J.; Wang, Z.; Zhou, W.; Kaliaguine, S. *J. Catal.*, **2004**, *227*, 242; (c) Sultana, A.; Nanba, T.; Haeda, M.; Sasaki, M.; Hamada, H. *Appl. Catal. B.*, **2010**, *101*, 61; (d) Martínez-Franco, R.; Moliner, M.; Concepcion, P.; Thogersen, J. R.; Corma, A. *J. Catal.*, **2014**, *314*, 73.
- [13] Martínez-Franco, R.; Moliner, M.; Thogersen, J. R.; Corma, A. *ChemCatChem*, **2013**, *5*, 3316.
- [14] Martinez-Franco, R.; Moliner, M.; Franch, C.; Kustov, A.; Corma, A. *Appl. Catal. B*, **2012**, *127*, 273.
- [15] Martínez-Franco, R.; Moliner, M.; Corma, A. *J. Catal.*, **2014**, *319*, 36-43.